Journal of Maps

ISSN: (Print) (Online) Journal homepage: https://www.tandfonline.com/loi/tjom20

High-resolution multibeam bathymetry of the northern Mid-Atlantic Ridge at 45–46° N: the Moytirra hydrothermal field

Luis Somoza, Teresa Medialdea, Francisco J. González, Sara Machancoses, Jose A. Candón, Constantino Cid, António Calado, Andreia Afonso, Luisa Pinto Ribeiro, Iker Blasco, Mónica Albuquerque, María Asensio-Ramos, Renato Bettencourt, Cristina De Ignacio, Enrique López-Pamo, Bruno Ramos, Blanca Rincón-Tomás, Esther Santofimia, Miguel Souto, Inês Tojeira, Cláudia Viegas & Pedro Madureira

To cite this article: Luis Somoza, Teresa Medialdea, Francisco J. González, Sara Machancoses, Jose A. Candón, Constantino Cid, António Calado, Andreia Afonso, Luisa Pinto Ribeiro, Iker Blasco, Mónica Albuquerque, María Asensio-Ramos, Renato Bettencourt, Cristina De Ignacio, Enrique López-Pamo, Bruno Ramos, Blanca Rincón-Tomás, Esther Santofimia, Miguel Souto, Inês Tojeira, Cláudia Viegas & Pedro Madureira (2021) High-resolution multibeam bathymetry of the northern Mid-Atlantic Ridge at 45–46° N: the Moytirra hydrothermal field, Journal of Maps, 17:2, 184-196, DOI: 10.1080/17445647.2021.1898485

To link to this article: https://doi.org/10.1080/17445647.2021.1898485

JOURNAL OF MAPS
2021, VOL. 17, NO. 2, 184–196
https://doi.org/10.1080/17445647.2021.1898485

SCIENCE

OPEN ACCESS Check for updates

High-resolution multibeam bathymetry of the northern Mid-Atlantic Ridge at 45–46° N: the Moytirra hydrothermal field

Luis Somoza [a], Teresa Medialdea [a], Francisco J. González [a], Sara Machancoses [b], Jose A. Candón [b], Constantino Cid [b], António Calado [c], Andreia Afonso [c], Luisa Pinto Ribeiro [c,i], Iker Blasco [a], Mónica Albuquerque [c], María Asensio-Ramos [d], Renato Bettencourt [e], Cristina De Ignacio [f], Enrique López-Pamo [a], Bruno Ramos [c], Blanca Rincón-Tomás [g], Esther Santofimia [a], Miguel Souto [c], Inês Tojeira [c], Cláudia Viegas [e,j] and Pedro Madureira [c,h]

[a]Marine Geology and Mapping Division, Geological Survey of Spain (IGME), Madrid, Spain; [b]Marine Hydrographic Institute, Spanish Navy (IHM), Cádiz, Spain; [c]Portuguese Task Group for the Extension of the Continental Shelf (EMEPC), Portugal; [d]Instituto Volcanológico de Canarias (INVOLCAN), Canary Islands, Spain; [e]IMAR- Instituto do Mar and Instituto de Investigação em Ciências do Mar – Okeanos da Universidade dos Açores, Horta, Portugal; [f]Complutense University of Madrid (UCM), Madrid, Spain; [g]Georg-August University Göttingen, Göttingen, Germany.; [h]Department of Geosciences and Institute of Earth Sciences, Évora University, Portugal; [i] GeoBioTec, Aveiro University, Aveiro, Portugal; [j]MARE – Marine and Environmental Sciences Center, Portugal

ABSTRACT

This work presents a new high-resolution multibeam bathymetric map of a segment of active deep sea-floor spreading in the Atlantic Ocean, the northern Mid-Atlantic Ridge (MAR) at 45–46º N. New high-resolution bathymetry data were acquired using an Atlas multibeam echosounder onboard the research vessel Sarmiento de Gamboa during the EXPLOSEA-2 survey in 2019. The final map of the MAR (50 m cell grid size) at the original scale of 1:200,000 shows a segment of 140 × 35 km of the MAR, at water depths from 715 to 3700 m. This new high-resolution bathymetric map allows to better defining the submarine morphology of the Moytirra hydrothermal active field, the only high-temperature field identified between the Azores Archipelago (Portugal) and Iceland. ROV submarine observations reaching the deepest part of the system for the first time show giant anhydrite-sulfide chimneys up to 20 m high, active strong black smokers and polymetallic massive sulfides.

ARTICLE HISTORY
Received 22 October 2020
Revised 25 February 2021
Accepted 1 March 2021

KEYWORDS
Multibeam bathymetry; Mid-Atlantic Ridge; Moytirra; hydrothermal vents; seafloor massive sulfides

1. Introduction

Mid-ocean ridges (MORs) constitute the lithospheric plate boundary where the oceanic crust, which covers 60% of the solid Earth's surface, is generated. MORs are linked to seafloor spreading and plates drift, and are thus features of first order importance in the Earth system. MORs illustrate well how volcanic, tectonic, hydrothermal and sedimentary processes sculpt geomorphology in the deep ocean (e.g. Mitchell, 2018; Searle, 2013). Despite their poor accessibility (lying 2700 m below sea level on average) and remoteness, the development and deployment of new technologies have been important for the discovery and investigation of new features on these geologic structures. Each ocean basin contains a MOR, and most of them are named for the basin they are in, as the Mid-Atlantic Ridge (MAR).

High-resolution seabed mapping is fundamental for the knowledge and understanding of deep-seafloor morphology, key geological processes, including sedimentary depositional and erosional processes, habitat distribution and typology and availability of mineral deposits and energy resources, among other aspects. It is also valuable for more applied purposes such as siting submarine cables and pipelines, detection of marine geohazards, development of early warning systems for volcanic eruptions, tsunamis and earthquakes, pollution prevention, fisheries management, analysis of potential environmental impacts associated with deep-sea exploration and exploitation, and for safer shipping.

Despite many years of mapping effort, only a small fraction of the world´s ocean seafloor has been sampled at a resolution higher than one nautical mile (one depth measurement every 1852 m), greatly limiting our ability to explore and understand critical ocean and seafloor processes (e.g. Ryan et al., 2009). Nevertheless, there are several recent international cooperation initiatives promoting seafloor mapping at high resolution. At global scale, the Nippon-Foundation GEBCO (The General Bathymetric Chart of the Oceans) Seabed 2030 has the goal of mapping

CONTACT Luis Somoza l.somoza@igme.es

the entire world´s ocean floor using Multi Beam Echo Sounders (MBES) data by 2030. The resolution of the global MBES seafloor mapping strongly depends on the water depth: 100 m resolution at water depths between 0 and 1500, 200 m resolution between 1500 and 3000, and 400 m resolution between 3000 and 4000 m (Mayer et al., 2018). The total coverage of ocean floor has significantly increased from 6% in 2014–15% in 2020 (https://www.gebco.net).

Otherwise, mapping seabed and habitat of the whole North Atlantic Ocean at high resolution is a challenge that is necessary to overcome the present knowledge on the Atlantic seabed. This task is being promoted by the Atlantic Seabed Mapping International Working Group (ASMIWG) as part of the Tri-Lateral Galway Statement agreed, between USA, European Union and Canada for the Atlantic Ocean Research Alliance (AORA, https://www.atlanticresource.org/aora/mapping-our-ocean).

The northern MAR is considered as a slow-spreading MOR with average spreading rates of 20–50 km Ma^{-1} (Lonsdale, 1977). Seawater penetrating the crust and heated by magma at depth creates hydrothermal spring in the way back to surface such as spectacular 'black smokers' and associated massive sulfide deposits (e.g. Mitchell, 2018). More than eleven high temperature vent fields have been confirmed in the axial valley of the MAR between the Equator and the Azores Archipelago (Portugal) at ~ 39° N (InterRidge Vents Database, https://vents-data.interridge.org/; Baker, 2017; Beaulieu et al., 2013).

However, between the Azores Archipelago and the Charlie-Gibbs Fracture Zone at 52° 25´ N, only one high-temperature hydrothermal field developing active black smokers has been reported at ~ MAR 45° N (Wheeler et al., 2013). In 2019 (11 June to 27 July 2019), the EXPLOSEA-2 survey (Somoza et al., 2020) aboard the RV *Sarmiento de Gamboa* carried out a complete seabed mapping of the axial valley of the segment of MAR where the Moytirra field was identified (Figure 1). Furthermore, the deepest part of the Moytirra hydrothermal field was surveyed for the first time down to the bottom of the MAR axial valley, at more than 3000 m water depth, using the ROV Luso, rated to 6000 m depth, whereas previously ROV used by the Irish-UK team was limited (Wheeler et al., 2013).

The northern MAR beyond the areas of national jurisdiction has been recently proposed by the International Seabed Authority (ISA) as a priority area for the development of a Regional Environmental Management Plan (REMP). REMPs have been interpreted as an essential tools, since they provide regional-specific information that facilitates the decision-making for present exploration and future exploitation of mineral resources in order to ensure the effective protection of the marine environment according to Article 145 of the United Nations Convention on the Law of the Sea (UNCLOS). In preparing the North Atlantic REMP, the procedure should involve the use of an extensive multidisciplinary scientific dataset including information such as high-resolution bathymetry mapping, habitat types, biodiversity, active vents, distribution and characterization of massive sulfide mineralizations as essential tools for ensuring the effective management and protection of the marine environment. The surveyed area is included in the extended continental shelf proposal submitted by Portugal to the United Nations Commission on the Limits of the Continental Shelf.

This work presents a new high resolution multibeam bathymetric map of a segment of the northern Mid-Atlantic Ridge (MAR) between 45° 20´ N and 46° 20´ N obtained during the EXPLOSEA-2 survey (http://www.igme.es/explosea), which includes the Moytirra active hydrothermal vent field, the only identified high-temperature hydrothermal field along the northern MAR between the Azores Archipelago and Iceland.

2. Methods

2.1. Acoustic data acquisition and processing

High-resolution bathymetry data were acquired using an Atlas DS 1 × 1 MBES onboard the RV *Sarmiento de Gamboa* during the EXPLOSEA-2 survey in 2019. The Atlas MBES operating at a frequency between 14 and 16 kHz, has an angular coverage of 140°, allowing a maximum of 360 beams per ping with an angular distance of 1° (Table 1). At average water depths of 1700 m, the real Atlas MBES coverage is four times the water depth with a resolution of 0.2% of the water depth. During the EXPLOSEA-2 survey we used a frequency of 15 kHz, a power of 236 dB, a pulse length of 30 ms, a gain of −132 dB and an average 313 beams per ping. The Atlas MBES collected bathymetry and backscatter data, together with water column data. We used the NAVIPAC (EIVA) navigation system to design bathymetric lines and to visualize 3D models of the multibeam bathymetry data in real time. Positioning was assured by a GPS system with an estimated error below 2 m.

MBES data were processed using CARIS HIPS&SIPS™ software. The MBES bathymetry data were used to generate digital terrain models (DTM) at spatial resolutions between 30 and 60 m. The multiresolution DTMs were also used to generate regional sun-shaded image renders and perspective views and to extract margin-wide bathymetric profiles using Fledermaus™ software to interpret the submarine landscapes. The rugosity map calculated in Fledermaus Version 7 is based on Jenness (2004) where rugosity is represented as the ratio between the surface and planar areas of each cell in the input bathymetric data set.

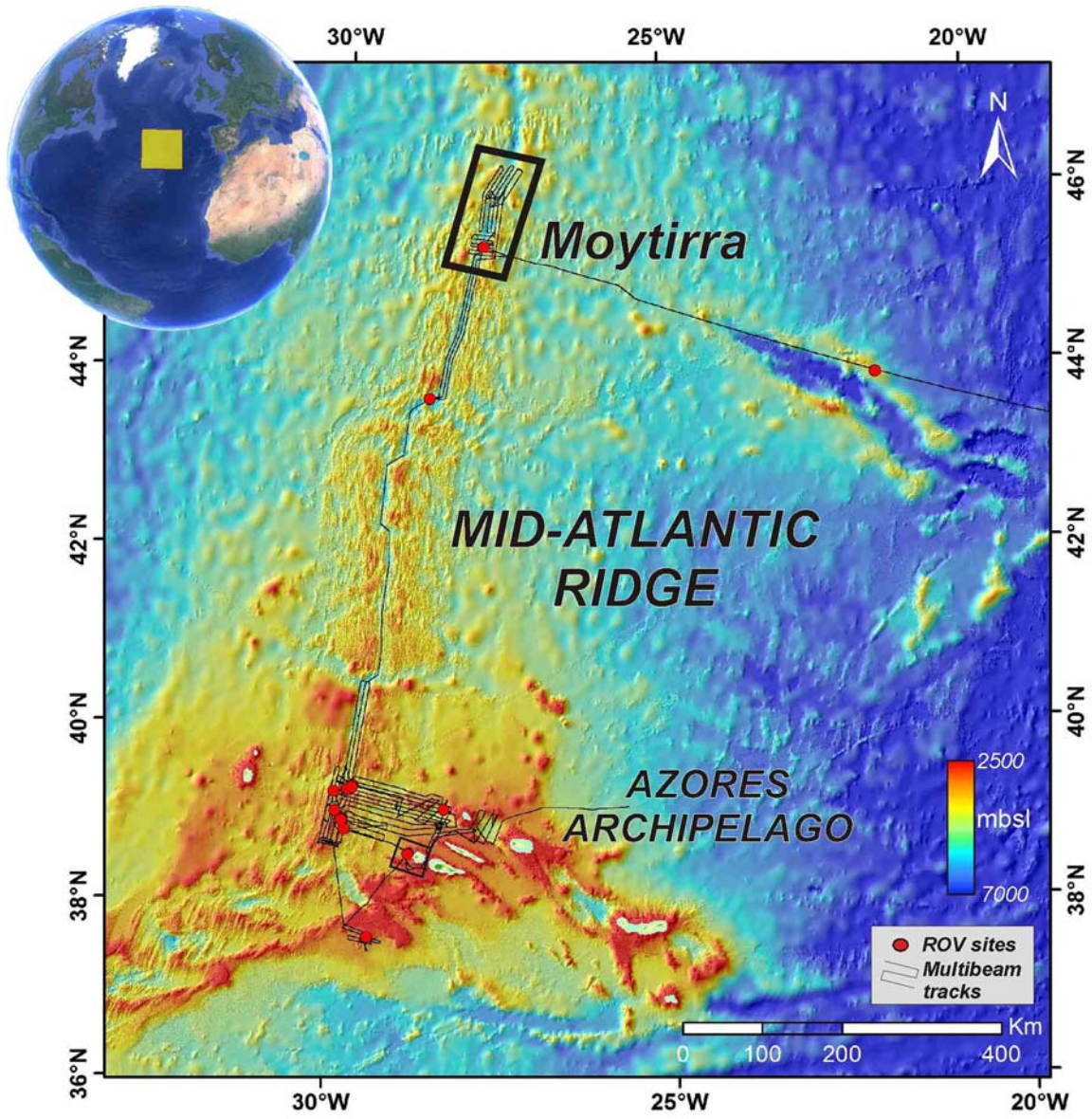

Figure 1. Location map of the surveyed areas along the northern Mid-Atlantic Ridge during the EXPLOSEA-2 survey (Somoza et al., 2020). The black rectangle marks the location of the mapped segment of the Mid-Ocean Ridge around the Moytirra hydrothermal field. ROV dive sites and multibeam tracks are also shown. Global Multi-Resolution Topography (GMRT) was used as regional background map (Ryan et al., 2009).

Table 1. Technical specifications for the multibeam system adopted in the survey.

Atlas DS 1×1 multibeam echosounder	
Frequency	14–16 kHz
Power	236 dB
Pulse length	30 ms
Gain	−132 dB
Along-track transmit beamwidth	1°
Across-track transmit beamwidth	1°
Max number of beams per ping	360
Average beams per ping	313
Angular coverage	140°
Coverage	4 times the depth at 1700 m
Total number of sounds (points)	332,673
Minimum depth	725.16 m
Maximum depth	3658.41 m
Average depth	2486.98 m
Standard deviation	451.49 m
Depth resolution	0.2 % of the water depth

DTMs were exported as ASCII ESRI files to ArcGis™ desktop v.12.4. ASCII ESRI files were transformed to raster files to generate derivative products such as slope angle maps in order to design the ROV tracks. In this way, Figure 2 shows the multi-resolution MBES data overlapped to Global Multi-Resolution Topography GMRT v3.7 bathymetric data available in this area (Ryan et al., 2009).

Sound Velocity Profiles (SVPs) used for correction of the MBES data consisted of real-time synthetic profiles derived from the CTDs data and Expendable Bathy Thermograph (XBT) probes T5, that were compared with the synthetic profiles from the WOA13 sound speed database (Masetti et al., 2018). Single beam bathymetric tracks were also collected using an EA600 echosounder in order to calibrate the gravimeter data. No further processing was applied to this data.

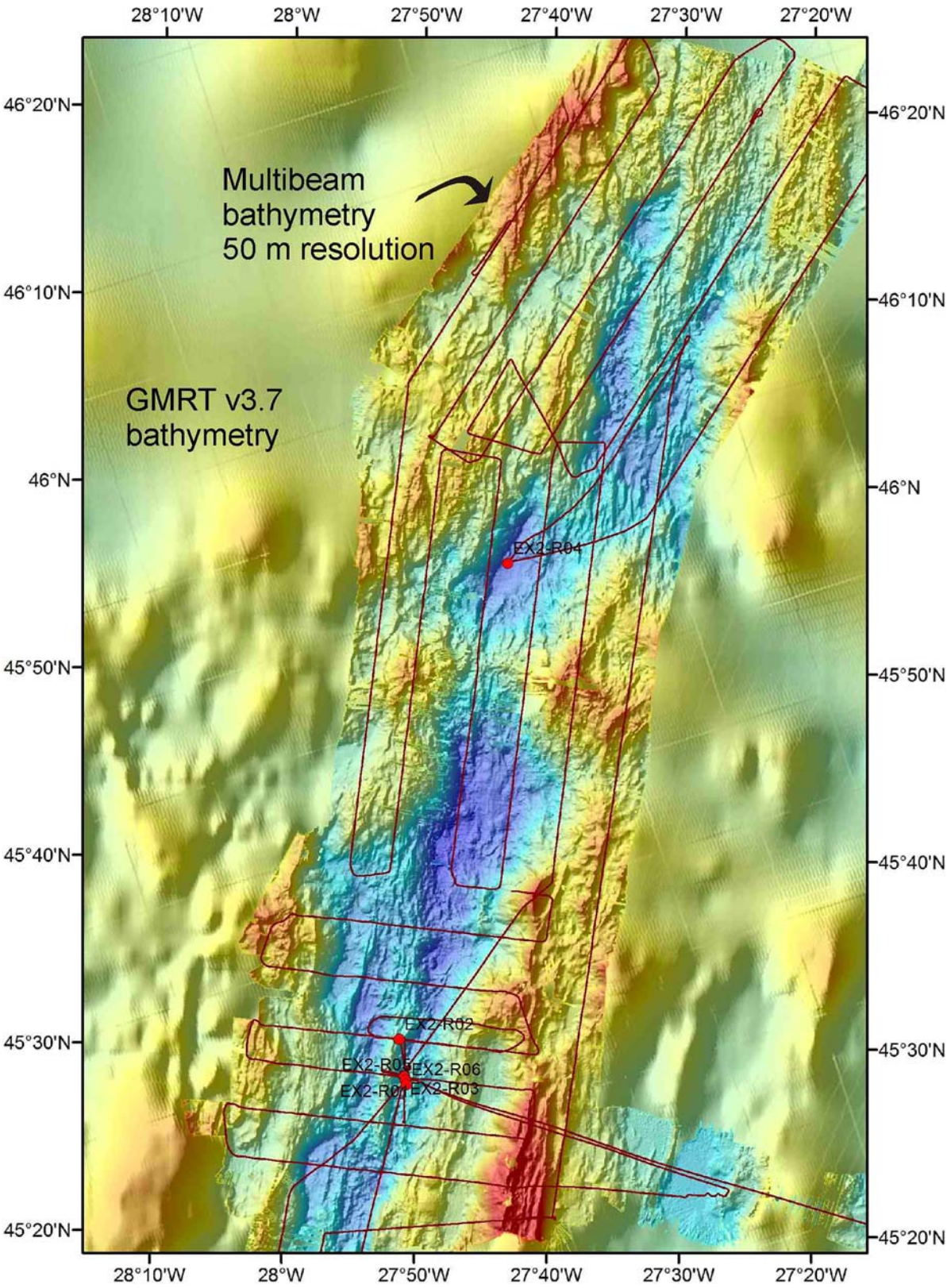

Figure 2. Multibeam bathymetry image obtained during EXPLOSEA-2 survey overlapped to Global Multi-Resolution Topography (GMRT) data produced using GeoMappApp (Ryan et al., 2009). Multibeam bathymetry tracks are also shown as red lines. Red dots mark location of CTDs casts for water column parameters measurements.

3. Results and discussion

All available data were merged to create a bathymetric map of the MAR drawn at the original scale of 1:200,000 in the segment between 45° 20′N and 46° 20′N which comprises the Moytirra active hydrothermal vent field (Figure 2 and **Bathymetric Map**). The final DTM of the MAR seafloor (50 × 50 cell grid size) shows an extension of 140 km of the MAR (Figure 3).

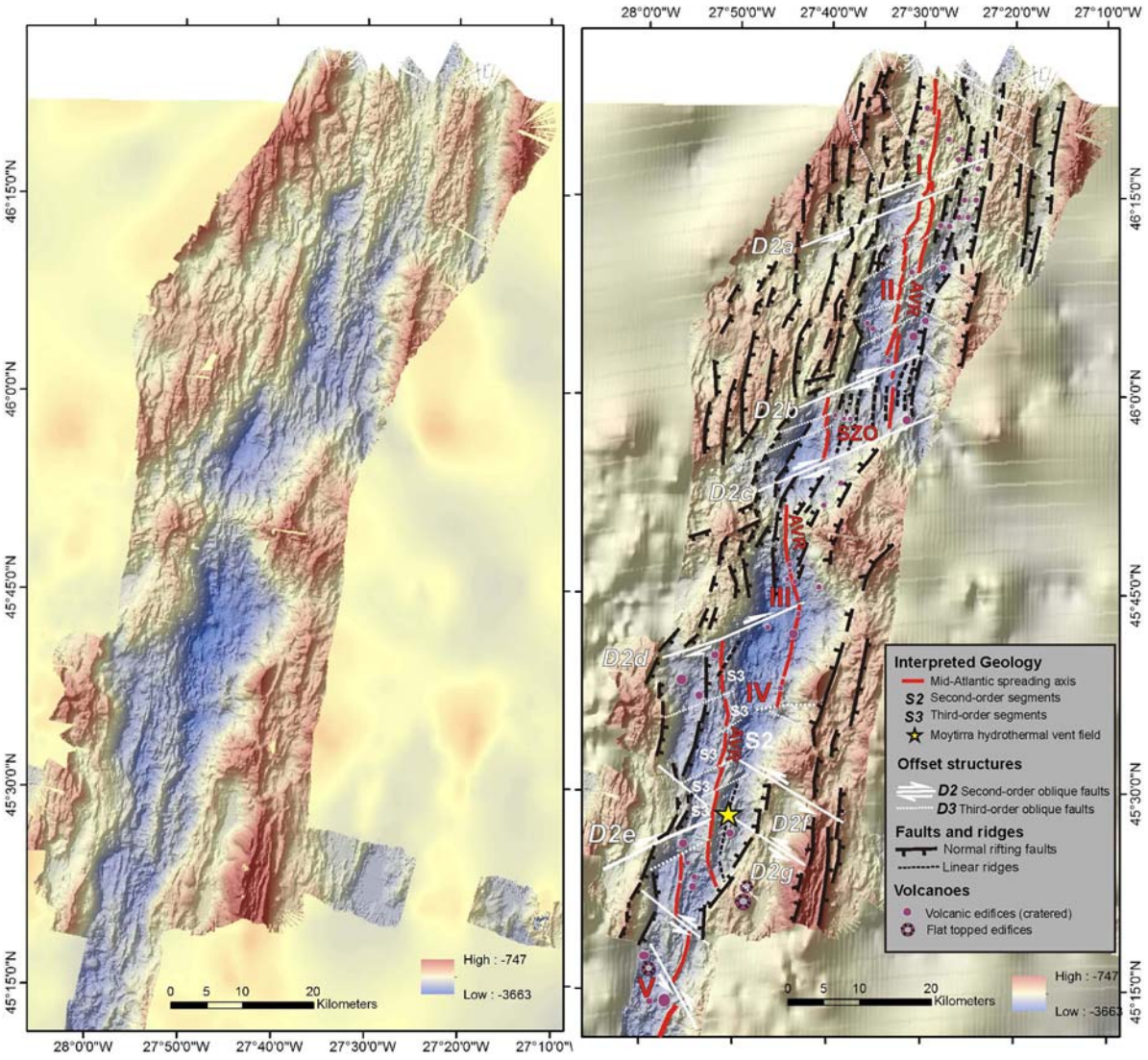

Figure 3. (left) Bathymetry and (right) interpreted geological map of the Mid-Atlantic ridge between 45° 10´N and 46° 30´N. AVR= Axial Volcanic Ridge; SZO= shear zone offset. Location in Figure 1. Projection UTM-28N.

3.1. Geological interpretation of the segmentation of spreading centers

Most of the MAR segments and other slow-spreading centers display an Axial Volcanic Ridge (AVR) aligned approximately normal to the spreading direction and containing the youngest lavas and a rugged topography (e.g. Searle, 2013). These AVRs are displaced by second-order and third-order discontinuities that take the form of oblique offsets (e.g. Searle & Laughton, 1977). The structural analysis of the high-resolution bathymetry map highlights the complexity of the spreading centers and ridge segmentation controlled by these systems of faults oblique to the spreading direction (Figure 3). The map legend used in the geological interpretation of the high-resolution map is based on the established classification of mid-ridge segmentation seafloor structures and volcanic geomorphology (e.g. Anderson et al., 2017; Macdonald et al., 1991; Searle, 2013) (Figure 4).

In the mapped area, we identified 5 segments along the mid-Atlantic spreading center that are between 26 and ~40 km long and ~9-20 km wide (Figure 3). These Individual segments are separated by second-order oblique faults (D2 in Figure 3), including major shear zones offsets (SZO), and numerous minor discontinuities (D3) according to the classification proposed by Macdonald et al. (1991) for discontinuities segmenting mid-ocean ridges. According this classification, D1 are the main transform faults, D2 corresponds to major oblique-slip normal faults offsetting between 5 and 9 km the second-order spreading segments (S2), and D3 are the minor oblique faults that only offset the axial volcanic valley forming third-order ridge segments (S3). The five segments identified can be grouped into northern (segments I and II) and southern (segments III, IV and V) ones separated by a complex shear zone offset (SZO in Figure 3) formed by a couple of D2 oblique slip normal faults, which offsets up to 9 km the axial ridge.

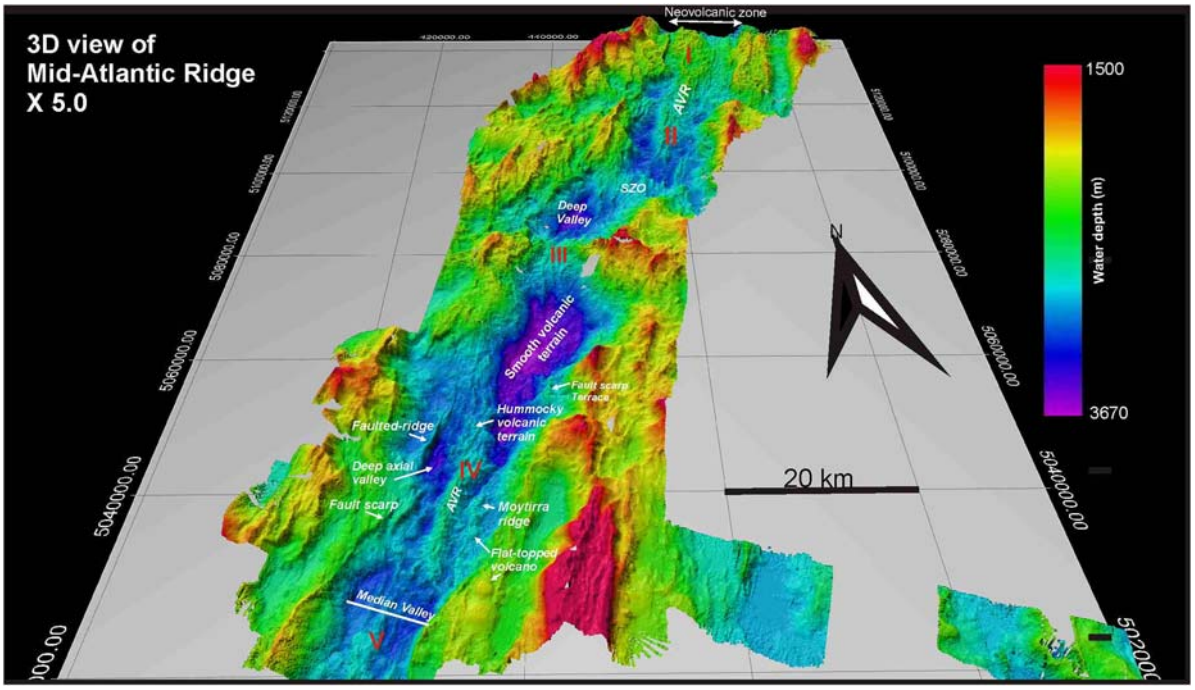

Figure 4. 3D views (x5) of the main physiographic domains along the MAR between 45° 10´N and 46° 30´N comprising the Moytirra active hydrothermal vent field. I to V labels the main ridge segments from north to south. AVR=Axial Volcanic Ridge. SOZ= Shear zone offset. I to V= Ridge segments. See text for details.

This system of D2 oblique-slip normal faults affects mainly the western side of the AVR showing mainly N-70° azimuths (Figure 3), whereas the eastern side of the southern AVR is only affected by a couple of also D2 faults trending N-120°. The western D2 system shows an angle of 70° oblique to the AVR whereas the eastern D2 system shows an angle of 60° oblique to the AVR. A third-order system of oblique-slip faults (D3) was identified affecting only the AVR and not its flanks. As occurs with the D2 faults, the D3 discontinuities show the same two main trends: N-70° and N ° 120°N. This type of discontinuities creates segmentation of S2 ridges generating S3 ridges as observed in segment IV (Figure 3).

3.2. Morphology types and volcanic edifices of the ridge segments

The northern segments (I and II), are 35-40 km long, 4 km wide and 400 m high, with the axial ridge located at the center of the median valley constituted by a depression of 10–12 km wide (Figure 5A). The axial ridge highs are at 2600 m water depth whereas the valley depressions go down to 3200 m. The slopes of the axial ridge show high gradients averaging 15–20°. Within the median valley of the northern segments, numerous sub-circular volcanoes and hummocky neovolcanic terrains are identified (Figures 3 and 5A). Hummocky ridges are believed to form from fissure eruptions where flow becomes unstable, breaking up into a line of small point sources (e.g. Searle et al., 2010). The median valley is bounded by steep fault scarps up 700 m high with slopes averaging up 20°. Terraces appear along the east edges of the median valley walls (Figure 5A).

The southern segments (III to V) vary from 26 to 37 km long, are 2 km wide and 500 m high, and are located at the center of the 8–12 km wide median valley (Figure 5B). Both, the axial ridge and the median valley are narrower than the northern ones (Figure 5B). The median valley is bounded by large fault scarps 800–1300 m high, forming terraces along their flanks. The eastern flank of the southern median valley shows the shallowest water depths of the area reaching values of 750 m. Along the intermediate terraces of segment IV in this eastern flank (Figure 5B), flat topped volcanoes with sub-circular morphology, 1200 m in diameter, 150 m height and steep slopes up to 25° are also identified. Flat topped volcanoes apparently form a distinct class of volcanoes, usually along slow spreading centers. Clague et al. (2000) proposed that they are formed by long-lived eruptions producing a lava lake and surrounding levee.

3.3. Morphology and structures controlling the Moytirra hydrothermal venting

The hydrothermal field of Moytirra is located at water depths between 2750 and 3060 m along the western flank of a ridge detached from the main eastern flank of segment IV (Figure 6). This ridge, which we termed as Moytirra ridge, extends ~10 km, in a sub-parallel

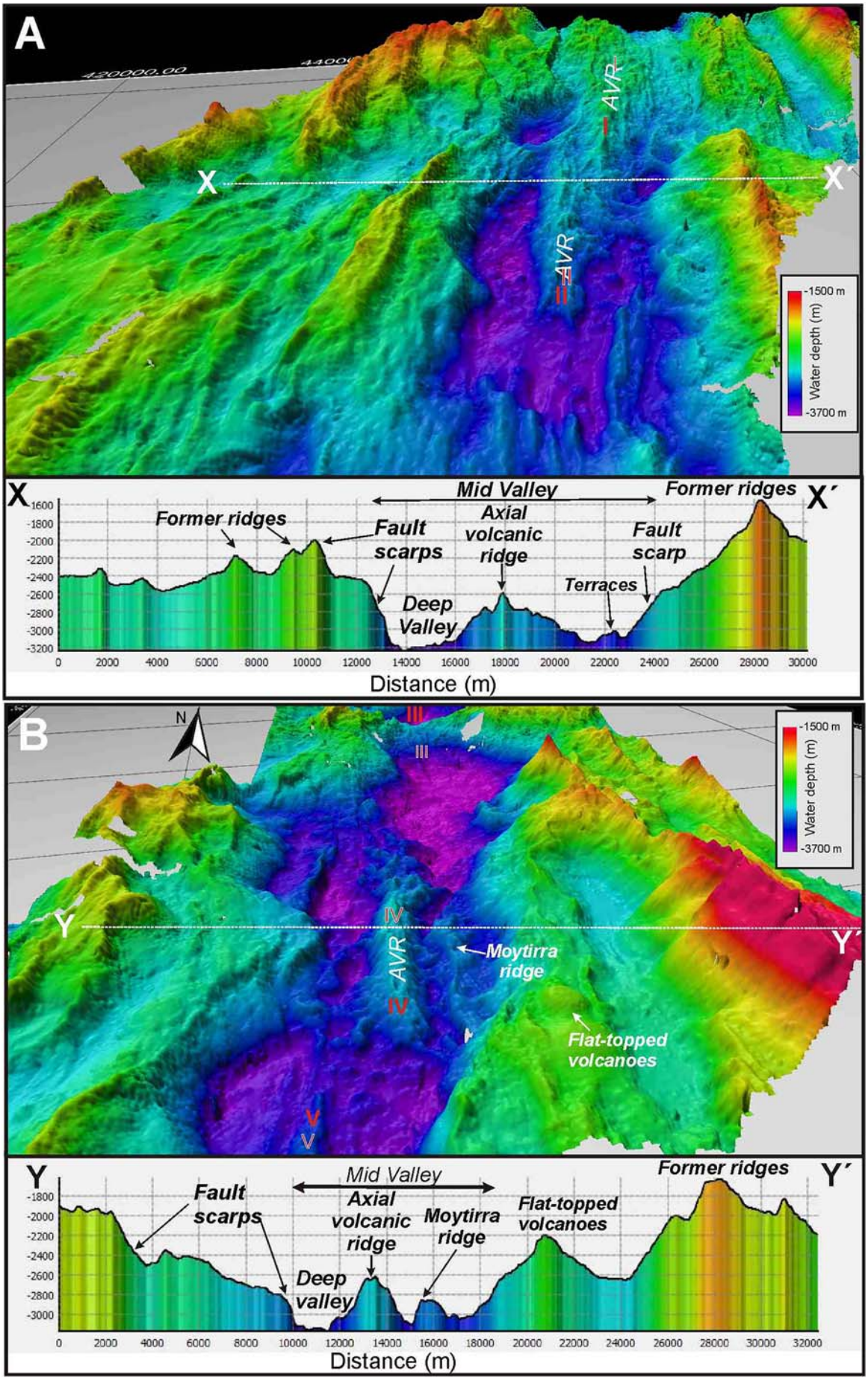

Figure 5. 3D views (x3) and transverse bathymetric profiles of the northern (A) and southern (B) segments of the MAR. AVR=Axial Volcanic Ridge. I to V= Ridge segments. See text for details.

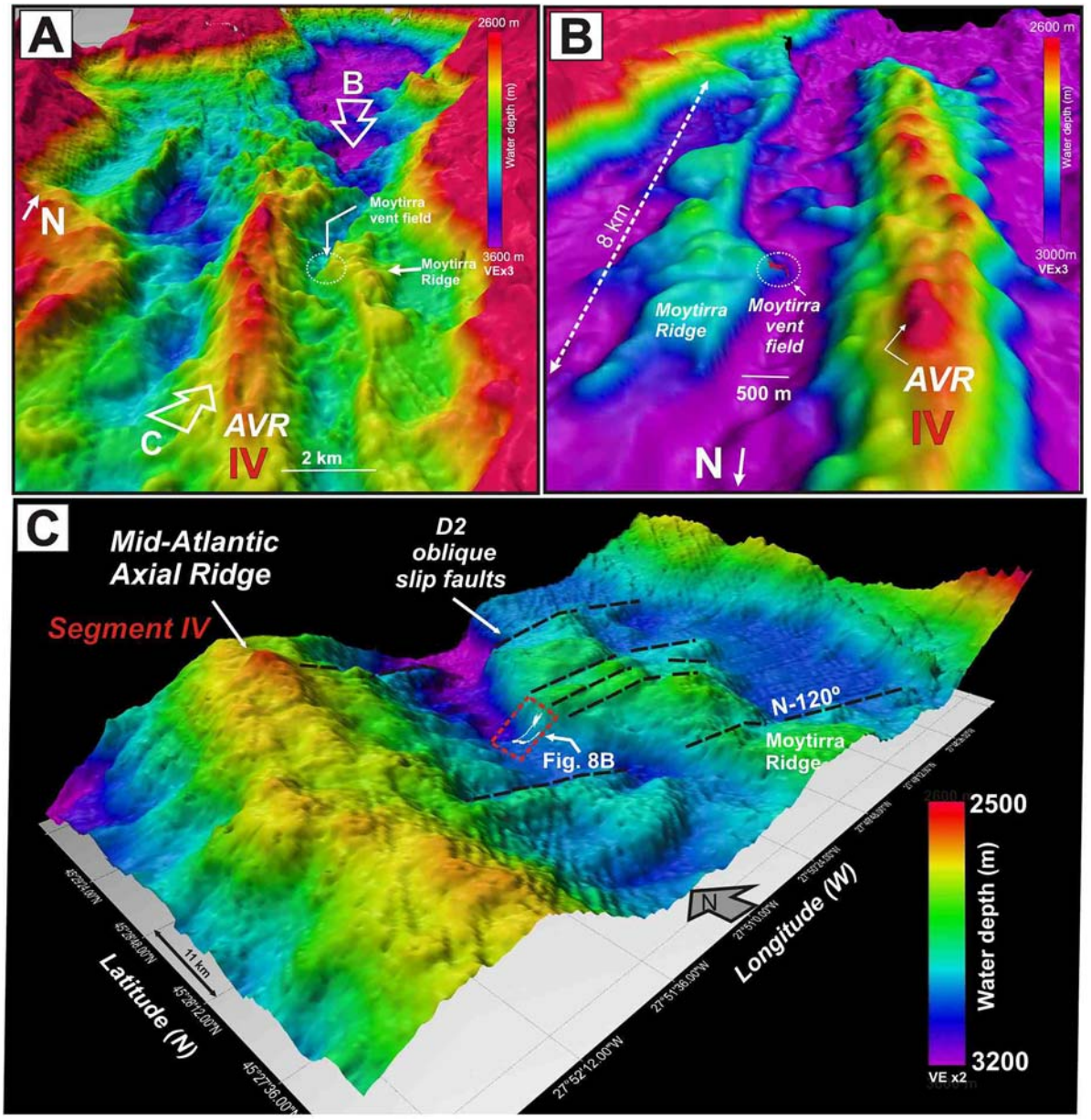

Figure 6. 3D views of the morphology Axial Volcanic Ridge (AVR) in the region of the Moytirra hydrothermal field: (A) View from the north; (B) View from the south; (C) Detail view of the segmentation of the Moytirra ridge by D2 oblique slip fault system. Red box shows the extension of the map of Moytirra hydrothermal field at 1:2000 scale showed in Figure 8(B). ROV tracks are marked by a white line. 3D grid at 30 m resolution. Note that water depth scale is different to emphasize the morphology of the ridge.

trend to the direction of the AVR but detached from the flanks of the median valley (Figure 6B).

The rugosity map of the Moytirra region shows that the Moytirra hydrothermal vent field is located at the intersection between D2 oblique faults with N-120° orientation and the eastern flank of the axial valley (Figure 7). At same time, the rugosity map shows that the Moytirra ridge is composed of a series of sub-circular structures interpreted as volcanic edifices (Figure 7).

The map of the Moytirra hydrothermal field at 1:2000 scale based on the observations from the ROV images shows the distribution of active and inactive chimneys as well as active black smokers along the field (Figure 8). The mapped area has an extension of ~24,000 cubic meters (Figure 8B). ROV observations showed that the active hydrothermal field is composed of an elongated mound of sea-floor massive sulfides topped by numerous anhydrite-sulfide chimneys up to 40 m high (Figure 9A) and active black smokers (Figures 9B,C). The active hydrothermal field extends ~125 m along a N-120° orientation covering an extension of ~5580 cubic meters (Figure 8B). The distribution of the cluster of chimneys fits with the orientation of the D2 oblique faults as observed on the rugosity map of the Moytirra region at regional scale (Figure 7). Furthermore, the uppermost boundary of the hydrothermal field is composed of steep walls of basalts showing evidence of fault planes. Based on these data, we interpret that Moytirra hydrothermal field develops from tensional gashes formed

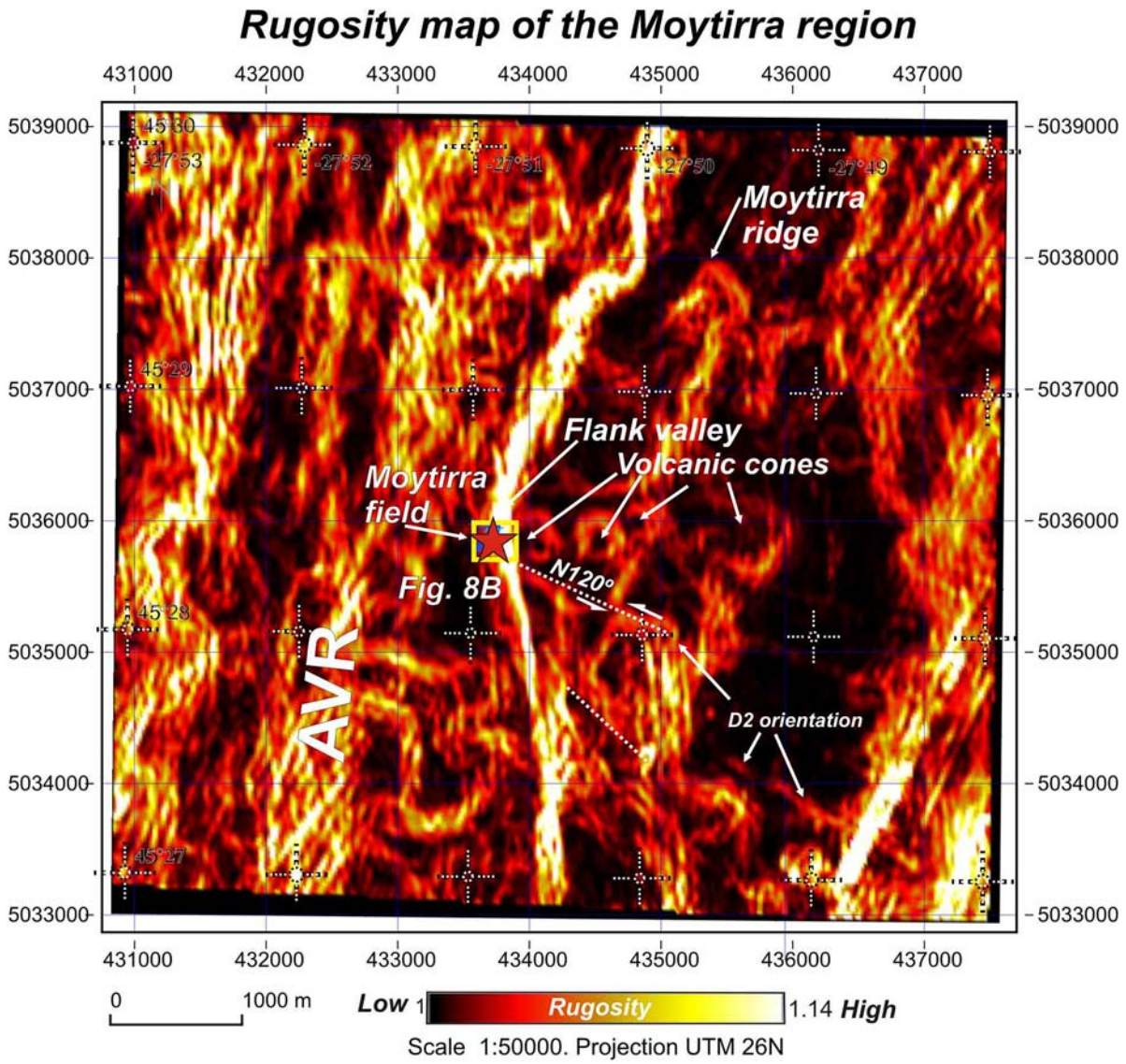

Figure 7. Rugosity map calculated from DEM multibeam bathymetry (30 m grid) showing main morpho-structures as D2 oblique faults and volcanic cones affecting the Moytirra Ridge. Location of the Moytirra hydrothermal field map at 1: 2000 scale shows in Figure 8(B) is marked by a yellow square. AVR: Axial Volcanic Ridge. Rugosity calculation using Fledermaus software according Jenness (2004).

by D2 oblique faults with N-120° orientation that intersect the flanks of the axial valley allowing fluids to rise at high-temperatures (Figure 8).

The active hydrothermal field is surrounded by a talus extending from 3000 to 3038 m water depths. This talus is constituted by blocks of weathered sulfide, variably covered by hemipelagic and hydrothermal sediments, forming chaotic talus of debris sourced from the destruction of the active vents. Hydrothermally extinct seafloor massive sulfide deposits forming chimneys and mounds also occur westwards at deeper waters from 3030to 3040 m (Figure 8B). This area is composed of an accumulation of weathered sulfides and iron-rich sediments with a discontinuous pelagic sedimentary cover. The talus of debris has a bulk extension of ~24,000 square meters (Figure 8B).

Processes of crustal accretion in the mapped segments of this slow-spreading mid-Atlantic ridge show certain similarities with back-arc ridges as the Mariana arc, both being characterized by strong ridge segmentation along shear zones offsets and non-transforms ridge-axis discontinuities (Anderson et al., 2017). In these slow-spreading mid-ocean ridges, second-order discontinuities take the form of oblique offsets in the spreading axis and median valley, such as occurs in the MAR at Kurchatov Fracture Zone (Searle & Laughton, 1977) and at 33.5° S (Grindlay et al., 1991). The main structures controlling ridge segmentation are these second-order systems of oblique-slip normal faults and tension gashes that offset the main segments of spreading ridges. Moreover, we interpret that active hydrothermal venting as the Moytirra field – is associated with the occurrence of these second-order oblique-slip normal faults (D2) as they intersect the outer flanks of the AVR, in contrast to back-arc ridges where hydrothermal venting is mainly associated with recent magmatism located along the axis of the AVR (e.g. Anderson et al., 2017).

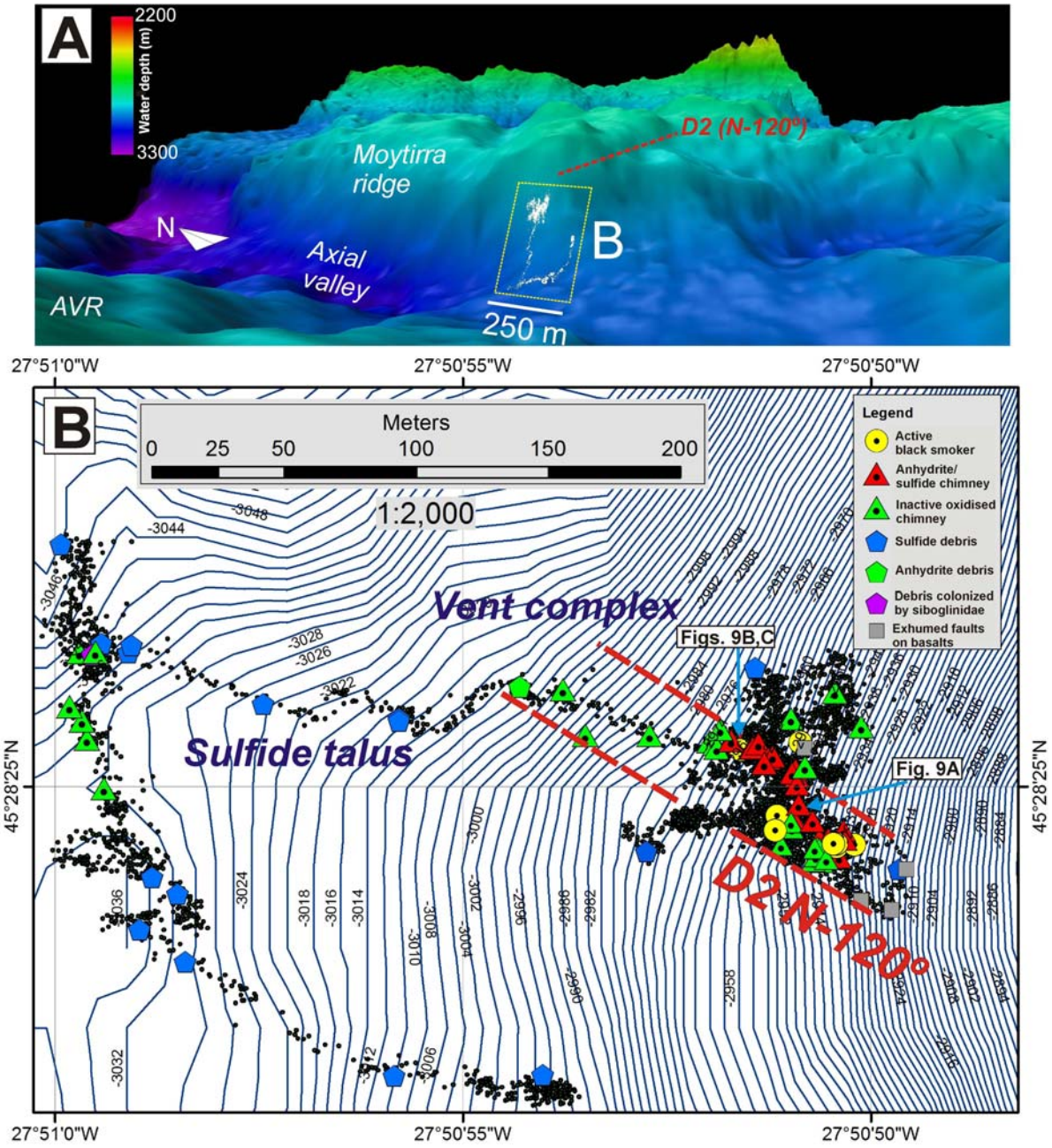

Figure 8. Map of the Moytirra hydrothermal field: (A) Location of the map (yellow square) and tracks of the ROV (white dots) along the flanks of the Axial Ridge Valley (AVR), (B) Map of the Moytirra hydrothermal field at 1:2000 scale based on the interpretation of ROV videos. Black dots are the filtered tracks of the ROV survey. Background bathymetry constructed from a grid at 30 m resolution. Bathymetric lines every 2 m. Map projection: Transverse Mercator Complex UTM Zone 26N. Location of images of sulfide/anhydrite chimneys and black smokers of Figure 9 are also indicated.

4. Conclusions

The new high-resolution bathymetric map presented here allows to better define the submarine morphology and structure of a segment up to 140 km in length of the northern MAR and their relationship with the occurrence of active hydrothermal vent fields and massive sulfide sites.

The morphological and geological interpretation of the high-resolution bathymetric map of the northern MAR between 45° 20´N and 46° 20´N which comprises the Moytirra active hydrothermal vent field allows to present the following conclusions:

- We identified 5 segments along mid-Atlantic spreading center that are between 26 and ~40 km long and ~9-20 km wide, offsets by second-order oblique slip normal faults (Figure 3). Two main orientations of these faults are identified: (a) a 70° trending system affecting mainly the western AVR; and (b) a 120° trending system affecting mainly the eastern AVR.
- The five segments identified can be grouped into northern (segments I and II) and southern (segments III, IV and V) ones separated by a WSW trending shear zone offset formed by a couple of

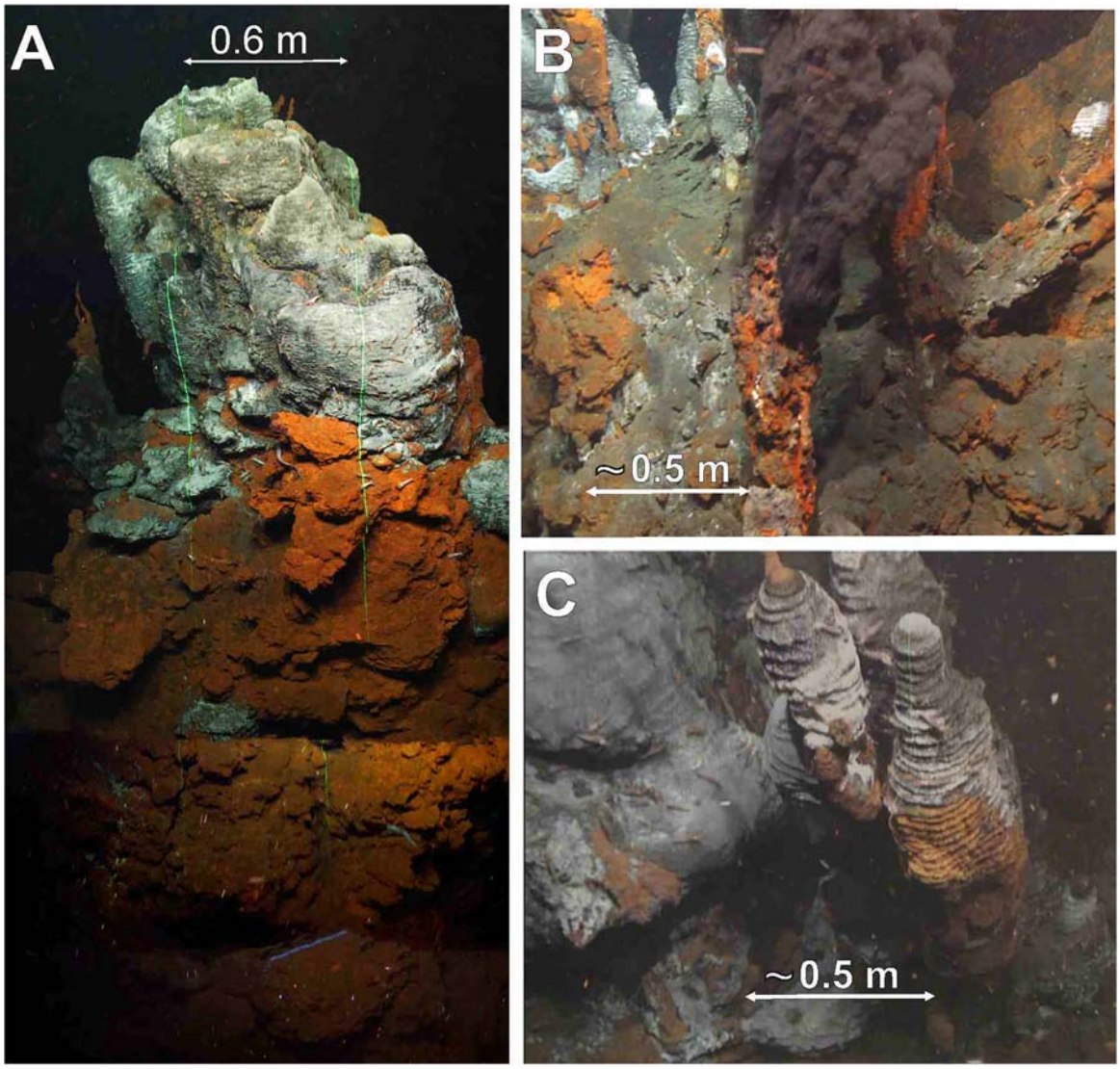

Figure 9. Images of the Moytirra hydrothermal vent field: (A) Image of anhydrite sulfide chimney up to 20 m high. Water depth: 2941 m. Location: 27° 50´ 51.270´´W, 45° 28´ 25.317´´N; (B) Active black smoker; Water depth: 2948 m. Location: 27° 50´ 51.540´´W, 45° 28´ 25.463´´N (C) Small anhydrite sulfide chimneys. Water depth: 2946 m. Location 27° 50´ 51.462´´W, 45° 28´ 25.462´´N. Location in Figure 8(B).

D2 oblique slip normal faults that offsets up to 9 km the axial ridge.

- The northern segments (I and II) of 35-40 km lenght are constituted by a ridge axis 4 km wide and 400 m high, and a median valley 10-12 km wide. These segments are characterized by numerous cratered sub-circular volcanic cones along the median valley. The median valley is bounded by step fault scarps up 700 m height with slopes averaging up 20°.
- The southern segments (III, IV and V) of 26-37 km length are constituted by a narrower ridge axis 2 km wide and 500 m high, located at the center of the 8–12 km wide median valley. These segments are characterized by flat-topped volcanic edifices located both on the median valley and along the flanks.
- The hydrothermal vent field of Moytirra, the only one discovered in the northern MAR between the Azores Archipelago and the Charlie-Gibbs Fracture Zone, is located along the western flank of a detached ridge of segment IV. This ridge, named here as the Moytirra ridge extents 8 km sub-parallel to the direction of the AVR.
- The field of active hydrothermal vents constituted by active black smokers and up to 20 m high anhydrite/sulfide chimneys located at 2915- 3000 m water depths extends ~125 m following a N-120° trend. The field of hydrothermal chimneys covers an area of ~5580 square meters. An apron of sulfide debris is located downslope at deeper waters from 3000 to 3050 m reaching the deepest ridge valley.
- Based on the geological interpretation of the high-resolution bathymetry at 1:200,000 scale (Figure 3), the rugosity map at 1:50,000 scale (Figure 7), and the detailed mapping of the distribution of active chimneys based on ROV observations at

1:2000 scale (Figure 8), we interpret that the Moytirra hydrothermal field is related to N-120° trending oblique slip-normal faults intersecting the steep flanks of the axial valley. We infer that these oblique faults are acting as tension gashes allowing fluids to circulate from the flanks of the former ridges to the AVR forming high-temperature fluid venting at the intersection with the flanks of the valley.

This study on the Moytirra hydrothermal site reached the deepest part of the system for the first time. The new bathymetric map of Moytirra segment of the MAR presented here, represents the basis for future investigation on the occurrence of further hydrothermal fields and seafloor massive sulfide sites along the Northern MAR.

Software

MBES data were processed using CARIS HIPS&SIPS™ software. Sound Velocity Profiles (SVPs) used for correction of the MBES data consist of real time synthetic derived from the CTDs data and Expendable Bathy-Thermograph (XBT) probes T5, that were compared with the synthetic profiles from the WOA13 sound speed database. Multi-resolution DTMs were also used to generate the Main Map and regional sun-shaded image renders and perspective views and to extract margin-wide bathymetric profiles using FLEDERMAUS™ software.

Acknowledgements

We are grateful to the Captain, the Officers and the Crew of the RV *Sarmiento de Gamboa* for their dedication during the EXPLOSEA-2 cruise. Special thanks to the technicians of the Unidad de Tecnología Marina (UTM, CSIC) including acoustic, seismic mechanics and computers, for their dedication and their professionalism during the cruise. Thanks to Hans van der Maarel, Bramley Murton and Melissa Anderson for their fruitful comments and suggestions in the review process of this work. LS: Chief Scientist of the Cruise, writing and overall organization. TM: Co-chief of the cruise and writing. SM, JAC, and CC: Onboard acquisition and process of the multibeam data. AC, AF, RB, BR, MS: ROV tracks, submarine positioning and 3D models. IB: Geographical information system (GIS) design. MA, IT, MAR, BRT and CV: Submarine image design and writing. FJG, LPR, CDI, ELP, ES and PM: Geological and petrological interpretation and writing.

Data availability statement

GIS data (multibeam tracks, CTDs and ROV stations) can be downloaded from the EXPLOSEA website at http://www.igme.es/explosea/dataset.html.

Disclosure statement

No potential conflict of interest was reported by the author(s).

Funding

The EXPLOSEA-2 cruise was funded by the Ministerio de Ciencia e Innovación of Spain as part of the project EXPLOSEA (CTM201675947-R, http://www.igme.es/explosea). The EXPLOSEA2 cruise benefit from the Scientific Agreement between Spain and Portugal to share oceanographic vessels and ROV. This study also benefits from the Atlantic Seabed Mapping International Working Group (ASMIWG) as part of the Atlantic Ocean Research Alliance Coordination and Support Action (AORA-CSA). This study is a contribution to the EMODNET-Geology project funded by the Executive Agency for Small and Medium-sized Enterprise (EASME/EMFF/2018/1.3.1.8-Lot 1/SI2.811048) and the GeoERA-MINDeSEA project funded by the Directorate-General for Maritime Affairs and Fisheries (Grant 731166, project GeoE.171.001). CV is supported by the Fundação para a Ciência e a Tecnologia (FCT) under the PhD fellowship (SFRH/BD/129683/2017) and strategic project (UIDB/05634/2020), PO2020 FunAzores (ACORES 01-0145-FEDER-000123) funded by the Azores Operational Program from European Regional Development Fund (ERDF), and H2020 SponGES project funded by the Horizon 2020 research and innovation program under grant agreement No. 679849.

ORCID

Luis Somoza http://orcid.org/0000-0001-5451-2288
Teresa Medialdea http://orcid.org/0000-0002-7969-5751
Francisco J. González http://orcid.org/0000-0002-6311-1950
Sara Machancoses http://orcid.org/0000-0002-0188-2506
Jose A. Candón http://orcid.org/0000-0002-3778-1301
Constantino Cid http://orcid.org/0000-0003-0285-5734
António Calado http://orcid.org/0000-0001-8525-2327
Andreia Afonso http://orcid.org/0000-0003-4906-0082
Luisa Pinto Ribeiro http://orcid.org/0000-0001-6529-9988
Iker Blasco http://orcid.org/0000-0002-3220-4636
Mónica Albuquerque http://orcid.org/0000-0003-0476-6436
María Asensio-Ramos http://orcid.org/0000-0002-8042-588X
Renato Bettencourt http://orcid.org/0000-0002-9223-3279
Cristina De Ignacio http://orcid.org/0000-0002-7250-5804
Enrique López-Pamo http://orcid.org/0000-0003-2177-3689
Bruno Ramos http://orcid.org/0000-0002-2283-4626
Blanca Rincón-Tomás http://orcid.org/0000-0003-1011-1508
Esther Santofimia http://orcid.org/0000-0003-4236-6812
Miguel Souto http://orcid.org/0000-0002-0822-5584
Inês Tojeira http://orcid.org/0000-0001-5778-6196
Cláudia Viegas http://orcid.org/0000-0003-4225-4167
Pedro Madureira http://orcid.org/0000-0003-4762-6273

References

Anderson, M. O., Chadwick Jr, W. W., Hannington, M. D., Merle, S. G., Resing, J. A., Baker, E. T., Butterfield, D. A., Walker, S. L., & Augustin, N. (2017). Geological interpretation of volcanism and segmentation of the Mariana back-arc spreading center between 12.7° N and

18.3° N. *Geochemistry, Geophysics, Geosystems*, *18*(6), 2240–2274. https://doi.org/10.1002/2017GC006813

Baker, E. T. (2017). Exploring the ocean for hydrothermal venting: New techniques, new discoveries, new insights. *Ore Geology Reviews*, *86*, 55–69. https://doi.org/10.1016/j.oregeorev.2017.02.006

Beaulieu, S. E., Baker, E. T., German, C. R., & Maffei, A. (2013). An authoritative global database for active submarine hydrothermal vent fields. *Geochemistry, Geophysics, Geosystems*, *14*(11), 4892–4905. https://doi.org/10.1002/2013GC004998

Clague, D. A., Moore, J. G., & Reynolds, J. R. (2000). Formation of submarine flat-topped volcanic cones in Hawai'i. *Bulletin of Volcanology*, *62*(3), 214–233. https://doi.org/10.1007/s004450000088

Grindlay, N. R., Fox, P. J., & Macdonald, K. C. (1991). Second-order ridge axis discontinuities in the south atlantic: Morphology, structure, and evolution. *Marine Geophysical Researches*, *13*(1), 21–49. https://doi.org/10.1007/BF02428194

Jenness, J. S. (2004). Calculating landscape surface area from digital elevation models. *Wildlife Society Bulletin*, *32*(3), 829–839. https://doi.org/10.2193/0091-7648(2004)032[0829:CLSAFD]2.0.CO;2

Lonsdale, P. (1977). Structural geomorphology of a fast-spreading rise crest: The east pacific rise near 3° 25′ S. *Marine Geophysical Researches*, *3*(3), 251–293. https://doi.org/10.1007/BF00285656

Macdonald, K. C., Scheirer, D. S., & Carbotte, S. M. (1991). Mid-ocean ridges: Discontinuities, segments and giant cracks. *Science*, *253*(5023), 986–994. https://doi.org/10.1126/science.253.5023.986

Masetti, G., Gallagher, B., Calder, B. R., Zhang, C., & Wilson, M. (2018). Sound speed manager: An open-source application to manage sound speed profiles. *The International Hydrographic Review*, *17*, 31–40.

Mayer, L., Jakobsson, M., Allen, G., Dorschel, B., Falconer, R., Ferrini, V., Lamarche, G., Snaith, H., & Weatherall, P. (2018). The Nippon foundation—GEBCO seabed 2030 project: The quest to see the world's oceans completely mapped by 2030. *Geosciences*, *8*(2), 63. https://doi.org/10.3390/geosciences8020063

Mitchell, N. C. (2018). Mid-ocean ridges. In A. Micallef, S. Krastel, & A. Savini (Eds.), *Submarine geomorphology* (pp. 349–365). Springer.

Ryan, W. B. F., Carbotte, S. M., Coplan, J. O., O'Hara, S., Melkonian, A., Arko, R., Weissel, R. A., Ferrini, V., Goodwillie, A., Nitsche, F., Bonczkowski, J., & Zemsky, R. (2009). Global multi-resolution topography synthesis. *Geochemistry, Geophysics, Geosystems*, *10*, 3, 1525–2027. https://doi.org/10.1029/2008GC002332

Searle, R. (2013). *Mid-ocean ridges* (p. 318). Cambridge University Press.

Searle, R. C., & Laughton, A. S. (1977). Sonar studies of the Mid-Atlantic Ridge and Kurchatov fracture zone. *Journal of Geophysical Research*, *82*(33), 5313–5328. https://doi.org/10.1029/JB082i033p05313

Searle, R. C., Murton, B. J., Achenbach, K., LeBas T., Tivey M., Yeo I., Cormier M.H., Carlut J., Ferreira P., Mallows C., Morris K., Schroth N., van Calsteren P., Waters C. (2010). Structure and development of an axial volcanic ridge: Mid-Atlantic Ridge, 45°N. *Earth and Planetary Science Letters*, *299*(1-2), 228–241. https://doi.org/10.1016/j.epsl.2010.09.003

Somoza, L., Medialdea, T., González, F. J., Calado, A., Afonso, A., Albuquerque, M., Asensio-Ramos, M., Bettencourt, R., Blasco, I., Candón, J. A., Carreiro-Silva, M., Cid, C., De Ignacio, C., López-Pamo, E., Machancoses, S., Ramos, B., Ribeiro, L. P., Rincón-Tomás, B., Santofimia, E., … Madureira, P. (2020). Multidisciplinary Scientific cruise to the northern Mid-Atlantic ridge and Azores archipelago. *Frontiers in Marine Science*, *7*, 568035. https://doi.org/10.3389/fmars.2020.568035

Wheeler, A. J., Murton, B., Copley, J., Lim, A., Carlsson, J., Collins, P., & Benzie, J. (2013). Moytirra: Discovery of the first known deep-sea hydrothermal vent field on the slow-spreading Mid-Atlantic Ridge north of the azores. *Geochemistry, Geophysics, Geosystems*, *14*(10), 4170–4184. https://doi.org/10.1002/ggge.20243